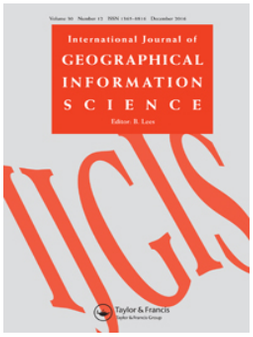

International Journal of Geographical Information Science

ISSN: 1365-8816 (Print) 1362-3087 (Online) Journal homepage: http://www.tandfonline.com/loi/tgis20

A universal spectral analytical method for digital terrain modeling

I. V. Florinsky & A. N. Pankratov

To cite this article: I. V. Florinsky & A. N. Pankratov (2016) A universal spectral analytical method for digital terrain modeling, International Journal of Geographical Information Science, 30:12, 2506-2528, DOI: 10.1080/13658816.2016.1188932

To link to this article: http://dx.doi.org/10.1080/13658816.2016.1188932

INTERNATIONAL JOURNAL OF GEOGRAPHICAL INFORMATION SCIENCE, 2016
VOL. 30, NO. 12, 2506–2528
http://dx.doi.org/10.1080/13658816.2016.1188932

Taylor & Francis
Taylor & Francis Group

A universal spectral analytical method for digital terrain modeling

I. V. Florinsky and A. N. Pankratov

Institute of Mathematical Problems of Biology, the Keldysh Institute of Applied Mathematics, Russian Academy of Sciences, Pushchino, Russia

ABSTRACT

There are three major mathematical problems in digital terrain analysis: (1) interpolation of digital elevation models (DEMs); (2) DEM generalization and denoising; and (3) computation of morphometric variables through calculating partial derivatives of elevation. Traditionally, these three problems are solved separately by means of procedures implemented in different methods and algorithms. In this article, we present a universal spectral analytical method based on high-order orthogonal expansions using the Chebyshev polynomials of the first kind with the subsequent Fejér summation. The method is intended for the processing of regularly spaced DEMs within a single framework including DEM global approximation, denoising, generalization, as well as calculating the partial derivatives of elevation and local morphometric variables.

The method is exemplified by a portion of the Great Rift Valley and central Kenyan highlands. A DEM of this territory (the matrix 480 × 481 with a grid spacing of 30″) was extracted from the global DEM SRTM30_PLUS. We evaluated various sets of expansion coefficients (up to 7000) to approximate and reconstruct DEMs with and without the Fejér summation. Digital models of horizontal and vertical curvatures were computed using the first and second partial derivatives of elevation derived from the reconstructed DEMs. To evaluate the approximation accuracy, digital models of residuals (differences between the reconstructed DEMs and the initial one) were calculated. The test results demonstrated that the method is characterized by a good performance (i.e., a distinct monotonic convergence of the approximation) and a high speed of data processing. The method can become an effective alternative to common techniques of DEM processing.

ARTICLE HISTORY
Received 14 February 2016
Accepted 8 May 2016

KEYWORDS
Chebyshev polynomials; Fejér summation; generalization; denoising; partial derivatives

1. Introduction

Topography is one of the main factors controlling processes taking place in the near-surface layer of the planet. In particular, topography is one of the soil forming factors since it influences: (a) climatic and meteorological characteristics, which controls hydrological and thermal regimes of soils; (b) prerequisites for gravity-driven overland and intrasoil lateral transport of water and other substances; and (c) spatial distribution of

CONTACT I. V. Florinsky iflor@mail.ru

vegetation cover. At the same time, being a result of the interaction of endogenous and exogenous processes of different scales, topography can reflect the geological structure of a terrain. In this connection, digital terrain analysis and digital terrain models (DTMs) are widely used to solve various multiscale problems of geomorphology, hydrology, remote sensing, soil science, geology, geophysics, geobotany, glaciology, oceanology, climatology, planetology, and other disciplines (Wilson and Gallant 2000, Li *et al*. 2005, Hengl and Reuter 2009, Florinsky 2012).

Mathematical issues of quantitative modeling and analysis of the topographic surface can be summarized in three major problems (Florinsky 2012):

(1) Interpolation of irregularly and regularly spaced digital elevation models (DEMs), bivariate discrete functions of elevation defining the topographic surface as a set of values measured at the grid nodes. This task is commonly carried out by various local interpolation methods (Schut 1976, Watson 1992, Mitas and Mitasova 1999, Hutchinson 2008).
(2) DEM filtering to denoise, generalize, and decompose DEMs into components of different spatial scales. These tasks can be attacked by 2D discrete Fourier transform (Papo and Gelbman 1984, Harrison and Lo 1996, Arrell *et al*. 2008), local quadratic approximation (Wood 1996), 2D discrete wavelet transform (Bergbauer *et al*. 2003, Bjørke and Nilsen 2003, Wu 2003), and 2D singular spectrum analysis (Golyandina *et al*. 2007).
(3) Derivation of local morphometric variables from regularly spaced DEMs. If the topographic surface is defined by a continuous, single-valued bivariate function

$$z = f(x, y), \tag{1}$$

where z is elevation, x and y are the Cartesian coordinates, local topographic variables are functions of the partial derivatives of elevation

$$p = \frac{\partial z}{\partial x}, \quad q = \frac{\partial z}{\partial y}, \quad r = \frac{\partial^2 z}{\partial x^2}, \quad s = \frac{\partial^2 z}{\partial x \partial y}, \quad t = \frac{\partial^2 z}{\partial y^2}, \ldots \tag{2}$$

For example, horizontal (k_h) and vertical (k_v) curvatures, one of the most important morphometric attributes, are calculated by the following equation (Shary 1995):

$$k_h = -\frac{q^2 r - 2pqs + p^2 t}{(p^2 + q^2)\sqrt{1 + p^2 + q^2}}, \tag{3}$$

$$k_v = -\frac{p^2 r + 2pqs + q^2 t}{(p^2 + q^2)\sqrt{(1 + p^2 + q^2)^3}}. \tag{4}$$

To compute p, q, r, s, and t (Equation 2) from DEMs on plane square grids or spheroidal equal angular grids, one can apply methods based on approximation of partial derivatives by finite differences using the 3 × 3 or 5 × 5 moving windows (Evans 1979, 1980, 2013, Zevenbergen and Thorne 1987, Shary 1995, Florinsky 1998, 2009, Minár *et al*. 2013).

Traditionally, these three key problems of digital terrain analysis are solved separately by means of procedures implemented in different methods and algorithms. Exceptions are very rare. For example, Mitášová and Mitáš (1993) developed a method for local interpolation of DEMs using regularized splines with tension, allowing simultaneous estimation of the partial derivatives of elevation (and, so, morphometric characteristics).

However, all three problems may be resolved within a single framework of DTM treatment based on the global approximation of a bivariate function by high-order (orthogonal) polynomials. In the 1960s–1980s, there were attempts to apply high-order polynomials for DEM global approximation (Heifetz 1964, Van Rossel 1972, Yagodina 1972, Segu 1985). These attempts have faced some challenges (McCullagh 1988, p. 753). First, global polynomial approaches by themselves have required considerable computer resources. Second, practical tasks have demanded to work with increasingly large DEMs containing tens of thousands to a few million points. Existed methods and computers could not handle such data amounts. As a result, an opinion was formed that the topographic surface is too complex for wide application of global polynomial approximations. The current prevailing view is that 'high quality global interpolation methods … are computationally impractical' for digital terrain modeling (Hutchinson 2008, p. 150). Only low-order (orthogonal) polynomials are utilized in trend-surface analysis, a technique to reveal trend and residual components of the topographic surface (Chorley and Haggett 1965, Tobler 1969, Davis 2002, ch. 5). However, progress in the theory and computational practice of polynomial approximation (Press *et al*. 1992, chs. 3–5, Dedus A.F. *et al*. 1995, Dedus F.F. *et al*. 1995, 1999, 2002, 2004, Britenkov and Pankratov 2004, Gautschi 2004, Pankratov and Britenkov 2004, Pankratov 2004a, 2004b, Pankratov *et al*. 2011, Kulikova 2007, Tetuev and Dedus 2007) as well as advances in computer technology suggest that the mentioned problems are no longer relevant.

In this article, we present a universal spectral analytical method based on high-order orthogonal expansions using the Chebyshev polynomials. The method is intended for the processing of regularly spaced DEMs within a single framework including DEM global approximation, denoising, generalization, as well as calculating the partial derivatives of elevation and local morphometric variables.

2. Method

Consider the function (Equation 1) defined in a rectangular domain. This function can be approximated using the bivariate Chebyshev series expansion (Clenshaw and Hayes 1965, Fox and Parker 1968, § 6.22):

$$z(x,y) = \sum_{i=0}^{l-1} \sum_{j=0}^{l-1} c_{ij} T_i(x) T_j(y), \tag{5}$$

where c_{ij} are expansion coefficients; $T_i(x)$ and $T_j(y)$ are the Chebyshev polynomials of the first kind in the variables x and y of degrees i and j, respectively; l is the maximum degree of expansion. It is assumed that the domain of the original function is translated into the domain of the orthogonal polynomials by a linear transformation.

The method can be described as consisting of four main stages: (1) calculation of expansion coefficients; (2) the Fejér summation; (3) reconstruction of the approximated function; and (4) calculation of derivatives. The 2D approximation of the original function (Equation 1) can be computationally performed as a superposition of two one-dimensional approximations by the variables x and y. So, below we describe the stages for the variable x only. For the variable y, the notations are mathematically identical.

Stage 1: Calculation of expansion coefficients. Let us apply numerical techniques for the approximation of a univariate function $u(x)$ using the Chebyshev series expansion (Press *et al*. 1992, § 5.8, Pankratov 2004a, 2004b):

$$u(x) = \sum_{i=0}^{l-1} c_i T_i(x), \tag{6}$$

where c_i are expansion coefficients; $T_i(x)$ are the Chebyshev polynomials of the first kind in the variable x of degree i; l is the maximum degree of expansion. The Chebyshev polynomials are defined as follows (Rivlin 1974, § 1.1):

$$T_i(x) = \cos(i \arccos x), \tag{7}$$

where $i = 0, \ldots, \infty$. We normalize the first polynomial of the function (Equation 7) so that $T_0(x) = \frac{1}{\sqrt{2}}$. This allows making the norm of each polynomial the same and equal to $\sqrt{\pi/2}$.

In the continuous form, the function $T_i(x)$ (Equation 7) satisfies the orthogonality condition under the scalar product:

$$\left(T_i, T_j\right) = \int_{-1}^{1} \frac{T_i(x)T_j(x)}{\sqrt{1-x^2}} dx = \begin{cases} 0 & \text{if} \quad i \neq j \\ \pi/2 & \text{if} \quad i = j \end{cases}, \tag{8}$$

where $i, j = 0, \ldots, \infty$.

In the discrete form, the orthogonality condition is also satisfied under the scalar product on a Gaussian quadrature grid of k nodes:

$$(T_n, T_m) = \frac{2}{k} \sum_{i=1}^{k} T_n(\xi_i) T_m(\xi_i) = \begin{cases} 0 & \text{if} \quad n \neq m \\ 1 & \text{if} \quad n = m \end{cases}, \tag{9}$$

where $n, m = 0, \ldots, k - 1$; ξ_i are nodes of the Gaussian quadrature grid:

$$\xi_i = \cos\left(\frac{\pi(i - 1/2)}{k}\right), i = 1, 2, \ldots, k \tag{10}$$

with k zeros of the orthogonal polynomial $T_k(x)$.

The expansion coefficients c_j can be calculated by the expression:

$$c_j = \left(u, T_j\right) = \frac{2}{k} \sum_{i=1}^{k} u(\xi_i) T_j(\xi_i). \tag{11}$$

where u is the original univariate function on the Gaussian quadrature grid; $j = 0, \ldots, l - 1$; $l \leq k$; round brackets in the central part of the expression denote the scalar product.

Stage 2: The Fejér summation. Approximations based on orthogonal polynomials always lead to oscillatory artifacts due to the Gibbs phenomenon (Jerri 1998, ch. 3, Florinsky 2002, § 2). In our case, this means that the Chebyshev series expansion (Equation 6) does not converge uniformly to the original function $u(x)$ at all points. According to the Fejér theorem, the arithmetic mean of the partial sums of the Fourier series of a continuous function converges uniformly to the function (Courant and Hilbert 1989, pp. 102–103, Jerri 1998, § 1.4). The Fejér theorem is also true for other orthogonal series (Jerri 1998, § 3.5). In other words, a uniform convergence of the approximation can be achieved replacing the initial expansion of $u(x)$ (Equation 6) by the arithmetic mean of the partial sums of the Chebyshev series:

$$\tilde{u}_n(x) = \frac{1}{n}\sum_{l=1}^{n} u_l(x), \tag{12}$$

where $\tilde{u}_n(x)$ is the Fejér sum. The Fejér summation is a powerful method to suppress oscillatory artifacts in polynomial approximation (Jerri 1998, Pankratov and Kulikova 2006).

In our case, the transformation of the expansion coefficients c_j, corresponding to the Fejér summation, has the form:

$$\tilde{c}_j = \frac{l-j}{l} c_j, \tag{13}$$

where $\tilde{c}_j$ are coefficients of an orthogonal series $\tilde{u}_n(x)$; $j = 0, \ldots, l-1$.

Stage 3: Reconstruction of the approximated function. Reconstruction of the original function is conducted by a simple summation of the orthogonal series. Generalization and/or denoising of the function are performed decreasing the number of expansion coefficients $\tilde{c}_j$ used for the reconstruction.

Stage 4: Calculation of derivatives. Let us calculate the first and second derivatives of the reconstructed function. For a Chebyshev-approximated univariate function, Press *et al*. (1992, § 5.9) described the calculation of the expansion coefficients of a derivative from the expansion coefficients of the original function. For an arbitrary basis, Tetuev and Dedus (2007, pp. 32–34) published a generalized conversion scheme for the expansion coefficients.

For the present case, the recurrence relations for the expansion coefficients c'_j of the first derivative of the orthogonal series are as follows:

$$\begin{cases} c'_{l-1} = 0 \\ c'_{l-2} = 2(l-2)\tilde{c}_{l-1} \\ \ldots \\ c'_j = c'_{j+2} + 2j\tilde{c}_{j+1}, \;\; j = l-3, \ldots, 0 \\ \ldots \\ c'_0 = \frac{c'_0}{\sqrt{2}} \end{cases}. \tag{14}$$

In the case of a linear transformation of function domain, expansion coefficients of the derivative should be scaled:

$$c'_j = \frac{2}{W} c'_j, \tag{15}$$

where W is the length of a function interval, $j = 0, \ldots, l-1$.

The expansion coefficients c''_j of the second derivative are calculated in the similar manner as c'_j (Equation 14):

$$\begin{cases} c''_{l-1} = 0 \\ c''_{l-2} = 2(l-2)c'_{l-1} \\ \dots \\ c''_j = c''_{j+2} + 2jc'_{j+1}, \;\; j = l-3, \dots, 0 \\ \dots \\ c''_0 = \frac{c''_0}{\sqrt{2}} \end{cases} . \tag{16}$$

The expansion coefficients of the *n*th order derivative can be similarly calculated.

After repeating the stages 1–4 for the variable *y*, we can obtain expressions for all partial derivatives of elevation in the form of the bivariate orthogonal series similar to Equation (5). For the first and second partial derivatives (Equation 2), the expressions are as follows:

$$p(x,y) = \sum_{i=0}^{l-1} \sum_{j=0}^{l-1} c_{ij}^p T_i(x) T_j(y), \tag{17}$$

$$q(x,y) = \sum_{i=0}^{l-1} \sum_{j=0}^{l-1} c_{ij}^q T_i(x) T_j(y), \tag{18}$$

$$r(x,y) = \sum_{i=0}^{l-1} \sum_{j=0}^{l-1} c_{ij}^r T_i(x) T_j(y), \tag{19}$$

$$s(x,y) = \sum_{i=0}^{l-1} \sum_{j=0}^{l-1} c_{ij}^s T_i(x) T_j(y), \tag{20}$$

$$t(x,y) = \sum_{i=0}^{l-1} \sum_{j=0}^{l-1} c_{ij}^t T_i(x) T_j(y), \tag{21}$$

where c_{ij}^p, c_{ij}^q, c_{ij}^r, c_{ij}^s, and c_{ij}^t are expansion coefficients for *p, q, r, s*, and *t*, respectively.

Now we can calculate values of the partial derivatives of elevation for all points of the reconstructed DEM by a simple summation of the related orthogonal series (Equations 17–21). Finally, to derive local morphometric variables, all the calculated values of the partial derivatives are substituted into the related expressions (e.g., Equations 3 and 4).

The described method can be used if one can ignore the planetary curvature within a DEM area. In other words, the diagonal length of a DEM rectangle should be less than at most 0.1 of the average radius of the planet.

3. Algorithm

To describe the algorithm implementing the method we use a polynomial-oriented matrix approach (Pankratov 2004b).

Let the original function of elevation z (Equation 1) be specified as an $m \times n$ matrix $\mathbf{A}$ with the elevation values at the nodes of a square grid; $x_1, \ldots, x_m$ and $y_1, \ldots, y_n$ are grid nodes in the interval [–1, 1] along the x- and y-axes, respectively; and $\xi_1, \ldots, \xi_k$ are nodes of the Gaussian quadrature grid.

The k values determine the maximum degree of expansion l in Equation (5), that is, $k \geq l$. Since $m \approx n$, the Gaussian quadrature grid is identical for the x- and y-axes. For a more accurate calculation of the expansion coefficients, it is recommended to choose the k value much greater than m and n: $k = N \cdot \max(m, n)$, $N \geq 8$.

Let us introduce the following notations: $\mathbf{L_{x\xi}}$ and $\mathbf{L_{y\xi}}$ are a $k \times m$ and $k \times n$ matrices of linear interpolation from the grids x and y, respectively, to the grid ξ; $\mathbf{T_\xi}$ is an $l \times k$ matrix of the Chebyshev polynomial values $T_i(\xi_j)$ in the grid ξ, where $i = 0, \ldots, l - 1$ and $j = 1, \ldots, k$; $\mathbf{F}$ is an $l \times l$ diagonal matrix with diagonal elements $(l - i)/l$ for the Fejér summation.

The calculation of the expansion coefficients of the elevation function is carried out in two steps. First, all columns of the matrix $\mathbf{A}$ are transformed into an $l \times n$ intermediate matrix of the expansion coefficients $\mathbf{C_y}$ that corresponds to the expansion in the variable y:

$$\mathbf{C_y} = \frac{2}{k}\mathbf{F}\mathbf{T}_\xi\mathbf{L_{y\xi}}\mathbf{A}. \tag{22}$$

Second, the matrix $\mathbf{C_y}$ is transposed and the transformation is repeated that corresponds to the expansion in the variable x:

$$\mathbf{C} = \frac{2}{k}\mathbf{F}\mathbf{T}_\xi\mathbf{L_{x\xi}}\mathbf{C_y}^{\mathrm{T}}, \tag{23}$$

where $\mathbf{C}$ is an $l \times l$ resultant square matrix of the expansion coefficients; $^{\mathrm{T}}$ denotes the matrix transpose.

Reconstruction of the approximated function is carried out by a summation of the orthogonal series:

$$\mathbf{Z} = \mathbf{T_x}^{\mathrm{T}}\mathbf{C}^{\mathrm{T}}\mathbf{T_y}, \tag{24}$$

where $\mathbf{Z}$ is an $m \times n$ matrix of the approximated values of the original function z (Equation 1) at the nodes of the square grid; $\mathbf{T_x}$ and $\mathbf{T_y}$ are an $l \times m$ and $l \times n$ matrices of the Chebyshev polynomial values $T_i(x_j)$ and $T_i(y_j)$ in the grids x and y, respectively.

Let $\mathbf{D}$ be an $l \times l$ differentiation operator in the space of expansion coefficients. In this case, $\mathbf{C_p}$, $\mathbf{C_q}$, $\mathbf{C_r}$, $\mathbf{C_s}$, and $\mathbf{C_t}$ – an $l \times l$ square matrices of expansion coefficients of the first and second partial derivatives p, q, r, s, and t (Equation 2) – are as follows:

$$\begin{aligned}
\mathbf{C_p} &= \mathbf{D}\mathbf{C}, \\
\mathbf{C_q} &= \left(\mathbf{D}\mathbf{C}^{\mathrm{T}}\right)^{\mathrm{T}} = \mathbf{C}\mathbf{D}^{\mathrm{T}}, \\
\mathbf{C_r} &= \mathbf{D}\mathbf{C_p}, \\
\mathbf{C_s} &= \left(\mathbf{D}\mathbf{C_p}^{\mathrm{T}}\right)^{\mathrm{T}} = \mathbf{C_p}\mathbf{D}^{\mathrm{T}}, \\
\mathbf{C_t} &= \left(\mathbf{D}\mathbf{C_q}^{\mathrm{T}}\right)^{\mathrm{T}} = \mathbf{C_q}\mathbf{D}^{\mathrm{T}}.
\end{aligned} \tag{25}$$

Reconstruction of the partial derivatives is carried out by a summation of the orthogonal series. For the first and second partial derivatives:

$$\begin{aligned}\mathbf{P} &= \mathbf{T}_\mathbf{x}^\mathrm{T}\mathbf{C}_\mathbf{p}^\mathrm{T}\mathbf{T}_\mathbf{y},\\ \mathbf{Q} &= \mathbf{T}_\mathbf{x}^\mathrm{T}\mathbf{C}_\mathbf{q}^\mathrm{T}\mathbf{T}_\mathbf{y},\\ \mathbf{R} &= \mathbf{T}_\mathbf{x}^\mathrm{T}\mathbf{C}_\mathbf{r}^\mathrm{T}\mathbf{T}_\mathbf{y},\\ \mathbf{S} &= \mathbf{T}_\mathbf{x}^\mathrm{T}\mathbf{C}_\mathbf{s}^\mathrm{T}\mathbf{T}_\mathbf{y},\\ \mathbf{T} &= \mathbf{T}_\mathbf{x}^\mathrm{T}\mathbf{C}_\mathbf{t}^\mathrm{T}\mathbf{T}_\mathbf{y},\end{aligned} \tag{26}$$

where **P, Q, R, S**, and **T** are an $m \times n$ matrices of the reconstructed values of the partial derivatives of elevation *p, q, r, s*, and *t* (Equation 2), respectively. Similar expressions are trivially deduced for the *n*th order partial derivatives.

4. Materials and data processing

To show the possibilities of the described method, we selected a portion of the East African rift system measuring 4° × 4° (about 442 × 442 km), located between 2°S and 2°N, and 35°E and 39°E (Figure 1). The area covers central and western regions of Kenya including a portion of the Great Rift Valley and central Kenyan highlands. A DEM of this territory was extracted from the global DEM SRTM30_PLUS (Sandwell *et al*. 2008). The DEM includes 230,880 points (the matrix 480 × 481); the grid spacing is 30″ (about 924 m) (Figure 2(a)).

First, using the finite-difference method (Florinsky 1998), we derived k_h and k_v models from the initial DEM (Figures 3(a) and 4(a)).

Second, we evaluated various sets of expansion coefficients to approximate and reconstruct DEMs. In particular, DEMs were reconstructed using 7000, 6000, 5000, 4000, 3400, 3000, 2880, 2400, 1920, 1200, 960, 480, 360, 240, 120, 60, and 30 expansion coefficients. Some of the sets of expansion coefficients were selected to illustrate capabilities of the method (Figure 2(b–f)). The first and second partial derivatives of

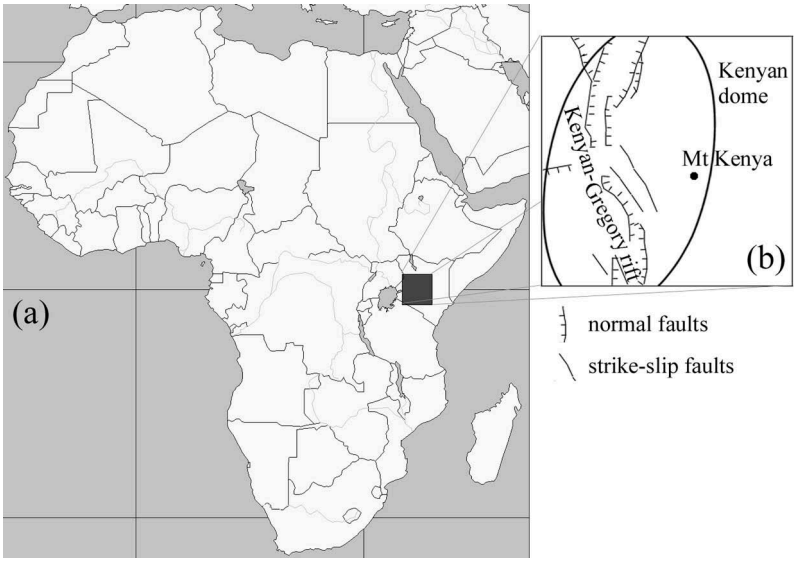

Figure 1. (a) Geographical location and the study area. (b) Key geological structures (Chorowicz 2005).

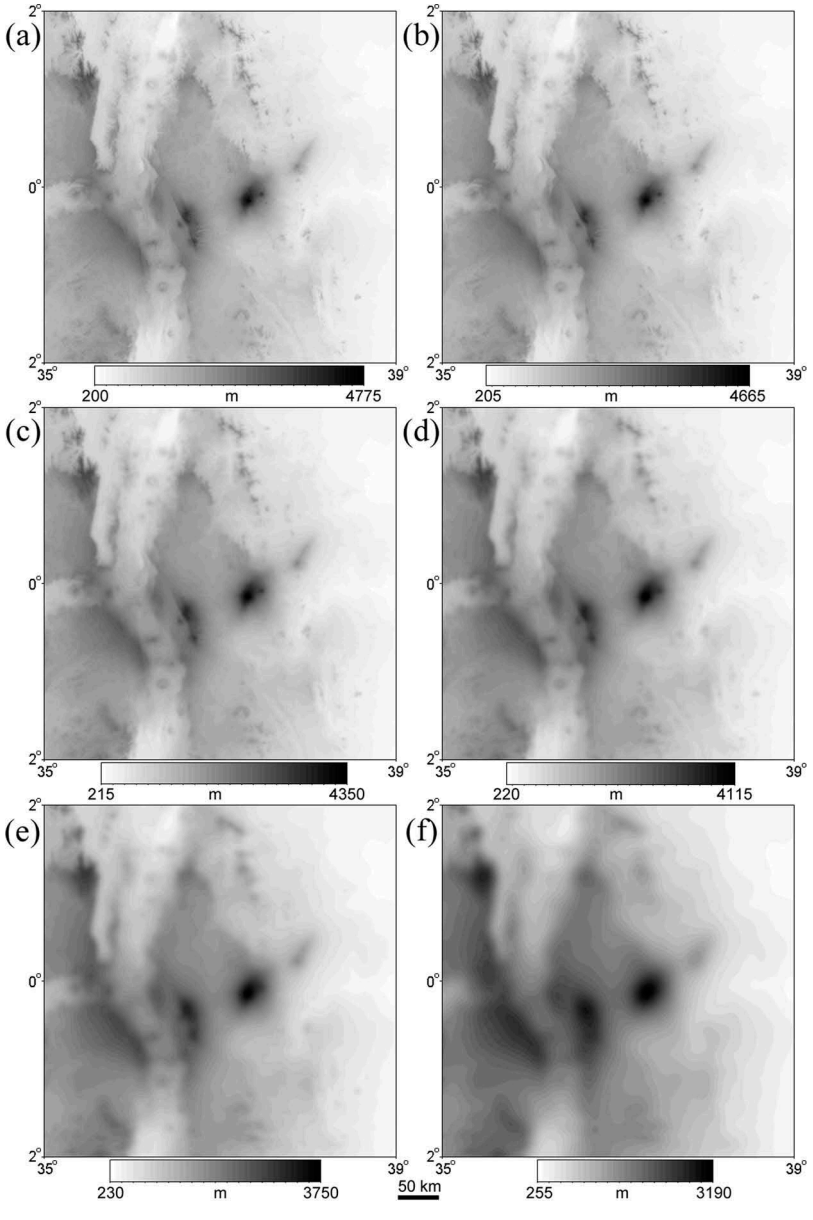

Figure 2. Kenya, elevations: (a) Initial DEM. Elevations reconstructed with: (b) 2880, (c) 480, (d) 240, (e) 120, and (f) 60 expansion coefficients.

elevation were calculated from each reconstructed DEM. Digital models of k_h and k_v were then computed using the derivatives (Figures 3(b–f) and 4(b–f).

Third, to evaluate the approximation accuracy, digital models of residuals – that is, differences between the reconstructed DEMs and the initial one – were calculated (Figure 5). Fourth, we performed a pairwise comparison of the reconstructed DTMs with the initial ones using samples extracted from each DTM. The sample size was 2209 points (the matrix 47 × 47); the grid spacing was 5′ (Figure 6). In this case, results of statistical

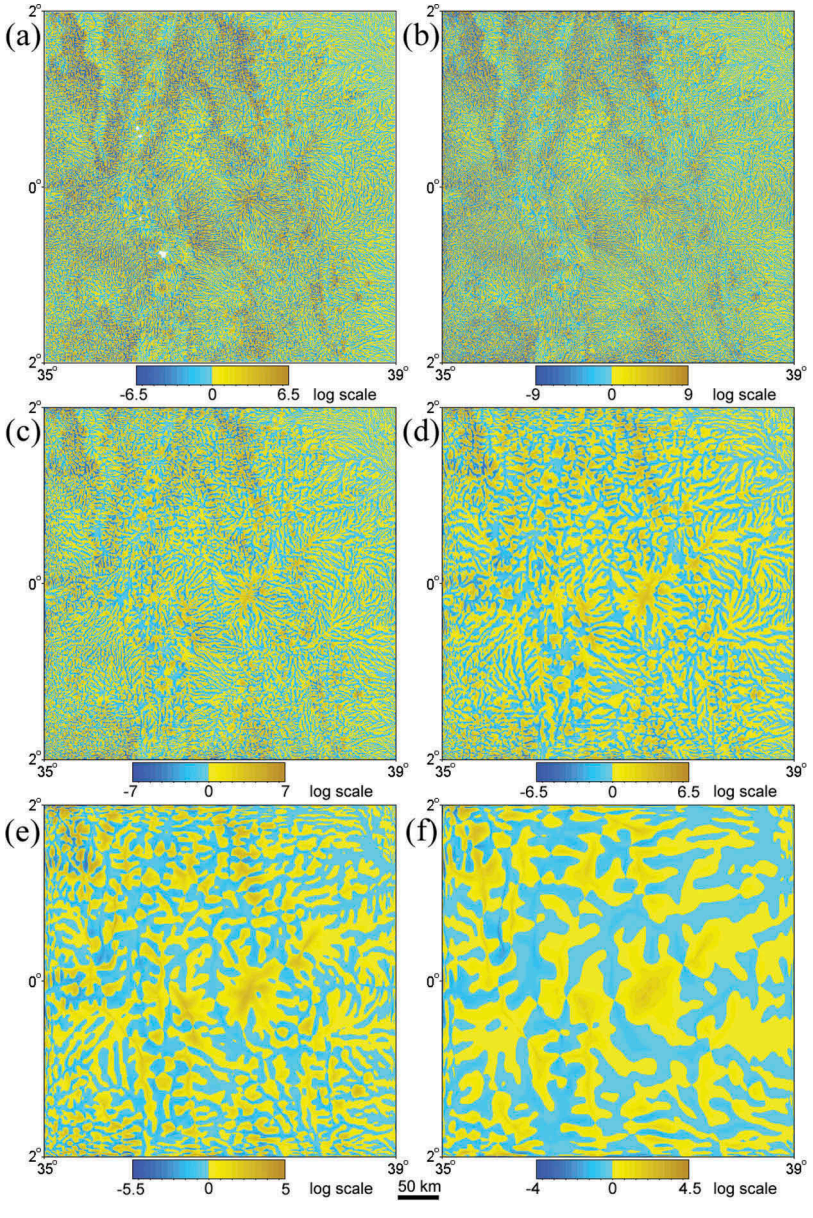

Figure 3. Kenya, horizontal curvature: (a) k_h derived from the initial DEM. k_h derived from reconstructed DEMs with: (b) 2880, (c) 480, (d) 240, (e) 120, and (f) 60 expansion coefficients.

estimations cannot be affected by the regular sampling associated with the DEM grid. This is because all mathematical procedures of the developed method are conducted on the Gaussian quadrature grid rather than the DEM grid (see details in Sections 2 and 3).

Fifth, to evaluate a role of the Fejér summation in the DTM treatment, we repeated DEM approximation as well as k_h and k_v derivation with the same sets of expansion coefficients, but without the Fejér summation (Figure 7). Digital models of residuals for the Fejér-free reconstructed DEMs were also calculated (Figure 8).

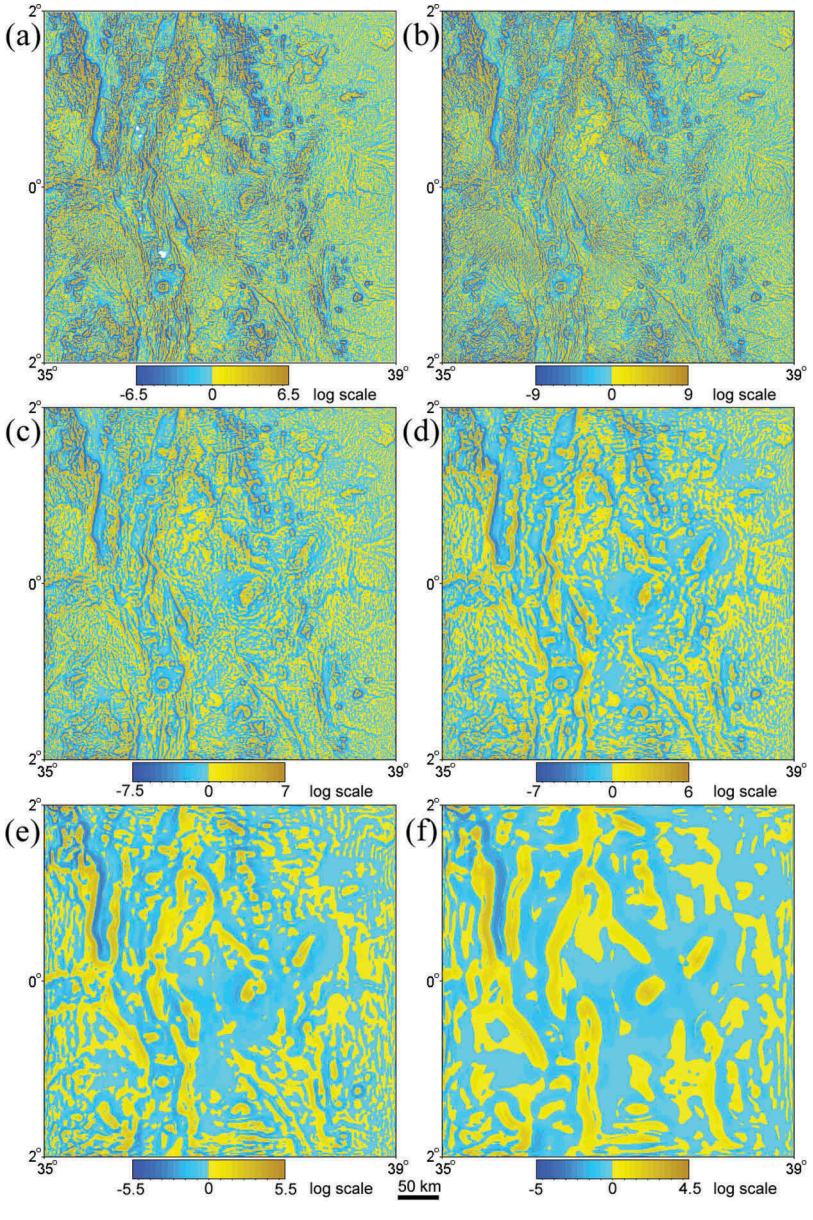

Figure 4. Kenya, vertical curvature: (a) k_v derived from the initial DEM. k_v derived from reconstructed DEMs with: (b) 2880, (c) 480, (d) 240, (e) 120, and (f) 60 expansion coefficients.

Finally, statistical characteristics of the residuals for the DEMs, reconstructed with and without Fejér summation, were obtained using samples from the digital models of residuals (Table 1). The sample size was 2209 points (the matrix 47 × 47); the grid spacing was 5′.

Wide dynamic ranges usually characterize topographic variables. To avoid loss of information on spatial distribution of values of morphometric attributes in mapping, it makes sense to apply a logarithmic transform using the following expression (Shary *et al.* 2002):

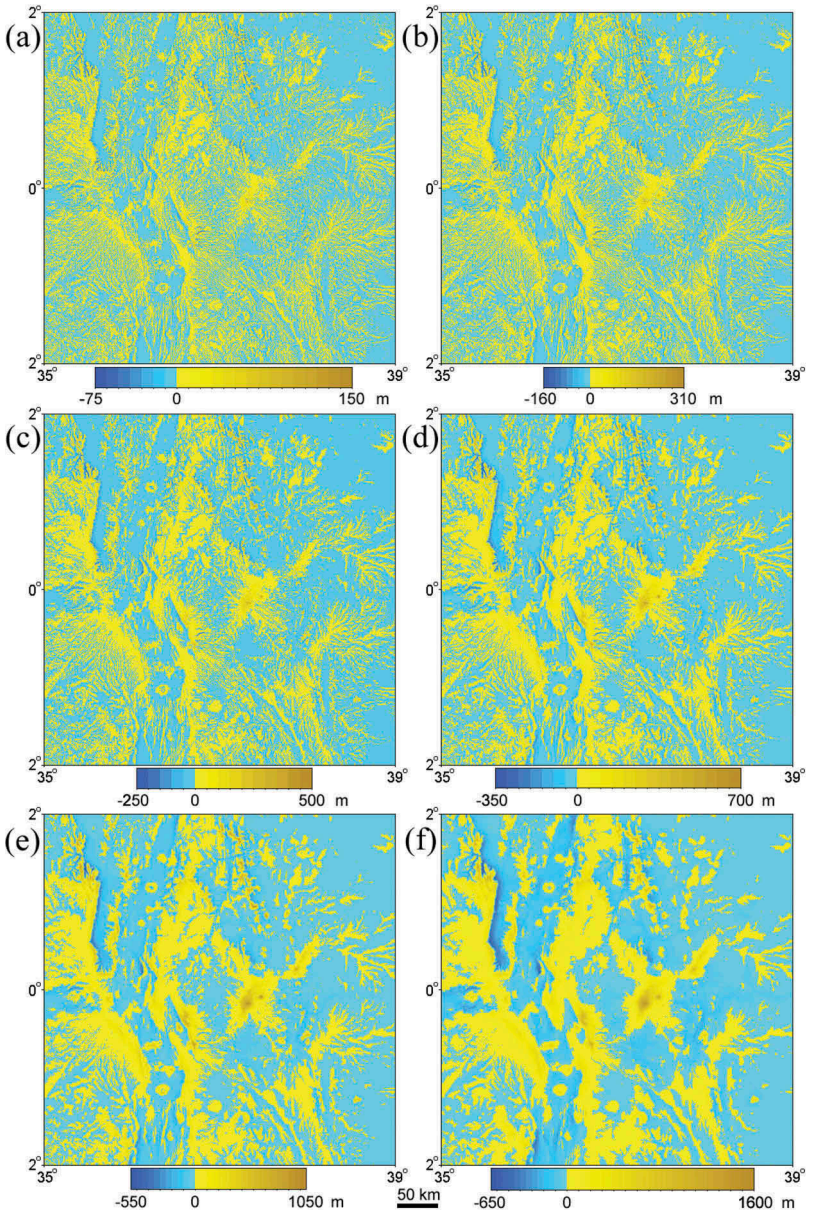

Figure 5. Residuals between the DEMs reconstructed with the Fejér summation and the initial DEM. Reconstructions were done with: (a) 2880, (b) 960, (c) 480, (d) 240, (e) 120, and (f) 60 expansion coefficients.

$$\Theta' = \mathrm{sign}(\Theta)\ln(1 + 10^n|\Theta|), \tag{27}$$

where Θ and Θ′ are an initial and log-transformed values of a morphometric variable, respectively; $n = 0$ for elevation and nonlocal variables, $n = 2,\ldots,18$ for local variables. Such a form of logarithmic transformation considers that dynamic ranges of some topographic attributes include both positive and negative values. Selection of the n

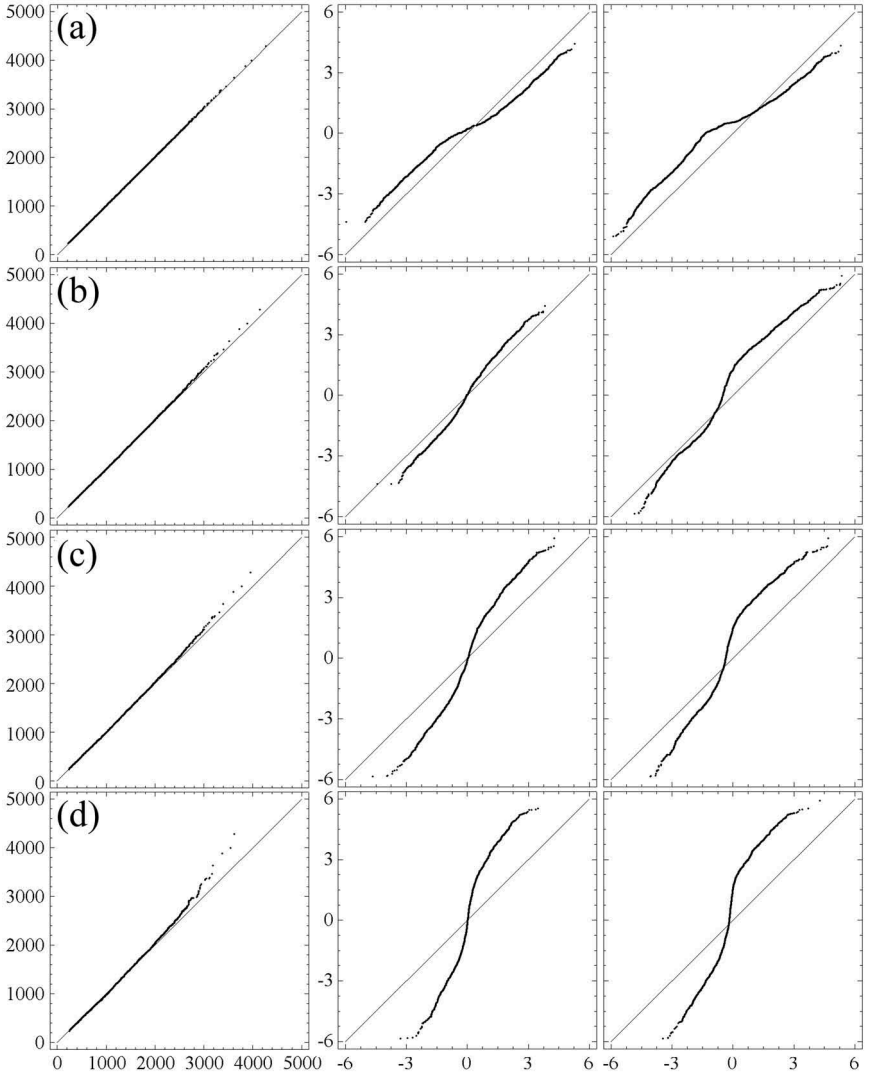

Figure 6. Quantile–quantile plots for elevation (left), k_h (center), and k_v (right) values, initial (*Y*-axis) and reconstructed (*X*-axis) with: (a) 2880, (b) 480, (c) 240, and (d) 120 expansion coefficients. The greater the distance between points and the diagonal line, the greater the difference between reconstructed and initial DTMs.

value depends on the size of a study area (Florinsky 2012, p. 134); we used $n = 6$ for k_h and k_v mapping (Figures 3, 4, and 7).

Data processing was done by the software MATLAB R2008b (© The MathWorks, Inc. 1984–2008). Statistical analysis was carried out with the software Statgraphics Plus 3.0 (© Statistical Graphics Corp. 1994–1997). Mapping was conducted with the software LandLord (Florinsky 2012, pp. 315–316).

To test the efficiency of the method in terms of the speed of data processing, we specially used an office computer with very modest capabilities (Intel Celeron, CPU G460, 1.80 GHz, 1.95 GB RAM) with MS Windows XP 32-bit edition. The test results are presented in Table 2.

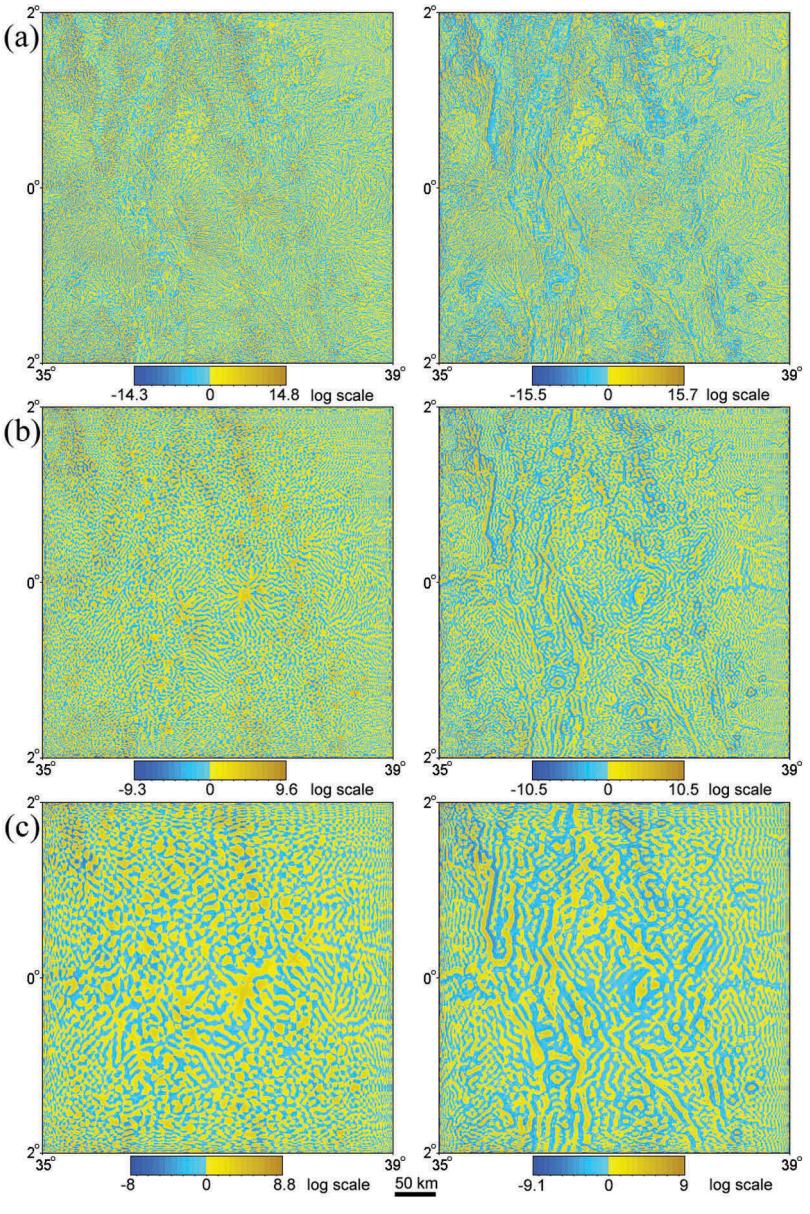

Figure 7. Examples of curvature maps – k_h (left) and k_v (right) – derived from the reconstructed DEMs without the Fejér summation using: (a) 2880, (b) 240, and (c) 120 expansion coefficients.

5. Results and discussion

A set of elevation maps reconstructed with different number of expansion coefficients (Figure 2) demonstrates a process of DEM generalization, from its zero level (Figure 2(a)) to the maximum one (Figure 2(f)). Similarly, a set of k_h and k_v maps calculated from reconstructed DEMs (Figures 3 and 4) shows k_h and k_v generalization, from the zero levels (Figures 3(a) and 4(a)) to the maximum ones (Figures 3(f) and 4(f)). Generally, the

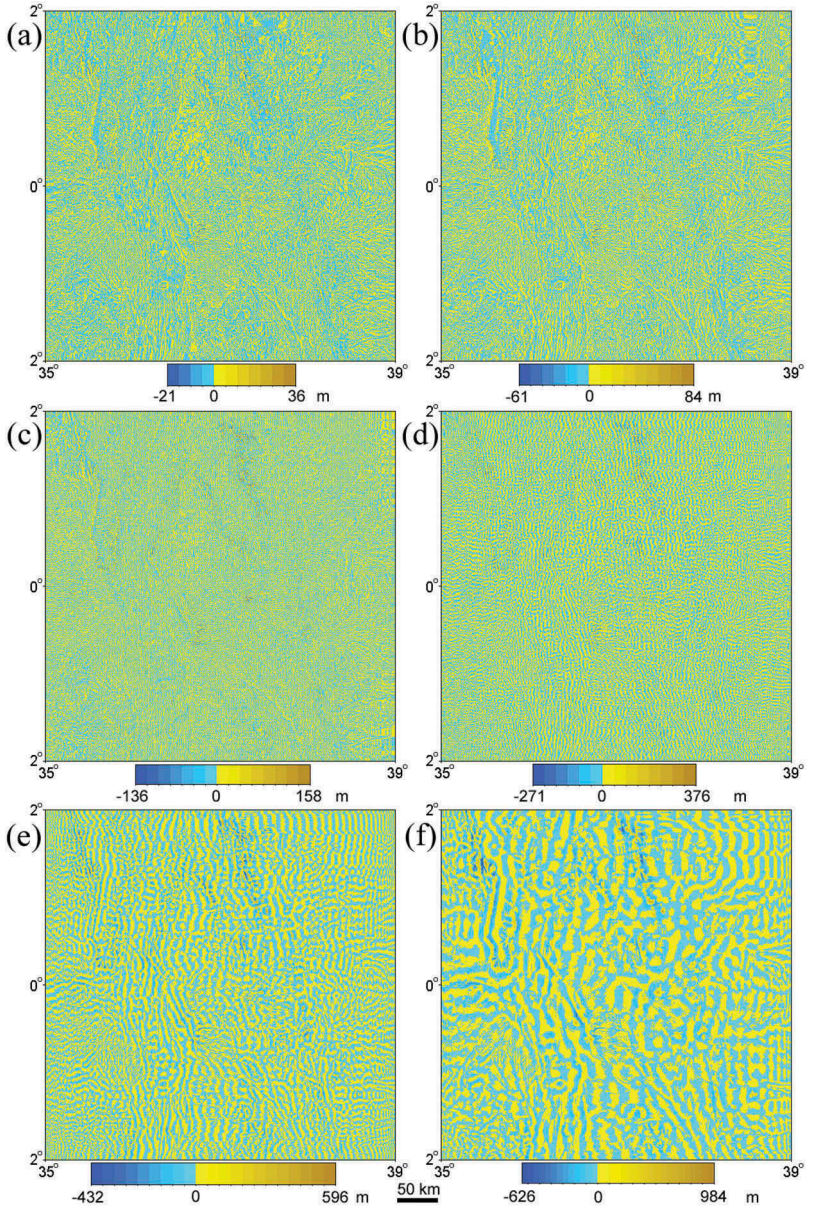

Figure 8. Residuals between the DEMs reconstructed without the Fejér summation and the initial DEM. Reconstructions were done with: (a) 2880, (b) 960, (c) 480, (d) 240, (e) 120, and (f) 60 expansion coefficients.

lower the number of expansion coefficients used to reconstruct a DEM, the more smooth and simplified maps obtained.

On the initial k_h and k_v map, one can find numerous flow structures descending from the Kenyan highlands to the coast of the Indian Ocean (Figure 3(a)) as well as scarps and terraces of the mountainous topography (Figure 4(a)). However, these non-generalized maps are overloaded with information. It is hard to see any generalization effect on

Table 1. Statistical characteristics of the residuals between the DEMs, reconstructed with and without Fejér summation, and the initial DEM.

	Number of expansion coefficients											
Statistics	60	120	240	480	960	1920	2880	3400	4000	5000	6000	7000
With the Fejér summation												
Minimum	−418.27	−287.46	−198.30	−146.08	−94.71	−57.51	−44.35	−39.97	−36.06	−31.54	−28.84	−28.20
Maximum	1163.49	669.29	427.11	265.23	158.20	90.72	64.26	55.43	48.49	41.61	37.50	36.09
Average	6.57	3.40	1.41	0.66	0.33	0.17	0.12	0.10	0.09	0.08	0.07	0.08
Standard deviation	131.69	84.94	53.50	32.94	20.19	12.07	8.83	7.75	6.82	5.72	4.97	4.47
Without the Fejér summation												
Minimum	−369.48	−251.56	−178.15	−80.92	−37.86	−20.73	−13.06	−13.41	−7.32	−8.47	−7.96	−5.38
Maximum	679.34	322.94	219.00	70.32	40.10	18.14	13.65	12.98	11.26	8.48	8.15	7.12
Average	0.45	−0.66	−0.37	0.03	−0.01	0.00	0.01	0.02	0.01	−0.02	−0.01	0.01
Standard deviation	69.58	42.46	24.12	11.48	5.29	2.74	1.83	1.63	1.31	1.05	0.89	0.80

The sample size is 2209.

Table 2. The average processing time to reconstruct a DEM and to calculate a morphometric variable depending on the number of expansion coefficients.

	Processing time, seconds	
Number of expansion coefficients	DEM reconstruction	Morphometric variable calculation
50	2.65	2.70
100	2.70	2.80
250	2.90	3.02
500	3.03	3.60
1000	3.78	5.26
1500	5.08	7.81
2000	6.59	11.14
2500	8.27	15.47
3000	10.74	20.70
4000	16.61	32.15
5000	23.68	–
6000	32.77	–
6500	38.40	–

maps calculated with 2880 expansion coefficients (cf. Figures 2(a,b), 3(a,b) and 4(a,b)). Readable and interpretable k_h and k_v maps were derived with 480, 240, 120, and 60 expansion coefficients: one can clearly see flow structures (Figure 3(c,d)), scarps, and terraces (Figure 4(c,d)), approximately north-striking large structures associated with elements of the Kenyan and Gregory rifts (Figure 4(e,f)), as well as some patterns probably connected with the evolution of the Kenya Dome (Figure 3(e,f)).

To avoid misunderstanding, we should stress that poor readability and interpretability of the low-generalized maps (Figures 3(b) and 4(b)) are associated with the particular scale of map representation. Zooming the low-generalized maps, it is possible to see complex systems of flow structures and other topographic features. These maps are not noisy; they are oversaturated with information, like the non-generalized maps of curvatures calculated by the traditional finite-difference method (Figures 3(a) and 4(a)).

The decrease in the number of the expansion coefficients in DEM reconstruction can act as high-frequency filtering. However, the visual analysis of the initial models of k_h and k_v (Figures 3(a) and 4(a)) shows that the initial DEM does not include a pronounced high-frequency noise, which would inevitably be increased after calculating derivatives and curvatures (Florinsky 2002). An example of the high-frequency filtering of a noisy DEM using our method can be found elsewhere (Florinsky and Pankratov 2015).

It is well-known that orthogonal polynomial approximation produces boundary effects, which cannot be completely eliminated. In our case, these effects appear as narrow linear artifacts at the boundaries of k_h and k_v maps (Figures 3(e,f) and 4(e,f)). A problem with boundaries of curvature maps also arises using the finite-difference algorithms: it is impossible to estimate the partial derivatives for boundary columns and rows of a DEM (Figures 3(a) and 4(a)), because they are estimated for the center point of the moving window (Evans 1979, Zevenbergen and Thorne 1987, Shary 1995, Florinsky 1998, 2009, Minár *et al*. 2013).

The analysis of Figure 5 shows that maximum residuals of the approximation predictably occur in areas of the contrast mountainous topography with dramatic elevation changes. However, an estimation of the approximation accuracy can be relevant only for DEMs reconstructed with a high number of expansion coefficients, for instance, with the set of 2880 coefficients (Figure 2(b)). In this particular case, the residuals range from –73

to 146 m (Figure 5(a)), while the original elevation ranges from 206 to 4774 m (Figure 2 (a)), that is, the range of calculation errors (219 m) is 4.8% of the elevation range in the initial DEM (4568 m). At the same time, the high residual values are typical for relatively small areas adjacent to the scarps of the Great Rift Valley, Mount Kenya, and the like. For most of the territory, the residuals are 0.1 ± 8.8 m (Figure 5(a) and Table 1). This value can be considered a permissible computational error, which is comparable with the vertical error of the initial DEM. Indeed, the land portion of the SRTM30_PLUS is based on the SRTM30 DEM (Becker *et al*. 2009) characterized by the absolute vertical error of 5–9 m for this part of Africa (Farr *et al*. 2007).

It is clear that the lower the number of expansion coefficients used to reconstruct a DTM, the greater the residual between a reconstructed DTM and the initial one (Figures 5 and 6). However, we purposely generalize the topographic surface reducing the number of expansion coefficients, so the approximation accuracy problem becomes irrelevant for generalized DEMs. In this case, the key criterion is a sufficient plausibility of reconstructed maps.

Figures 7–9 and Table 1 demonstrate the role of the Fejér summation in the developed method. On the one hand, although both approximation versions – with and without the Fejér summation – are characterized by a distinct monotonic convergence, the convergence rate of the Fejér-free approximation is markedly increased (Figure 9 and Table 1). For example, the residuals for the DEM reconstructed with the set of 2880 expansion coefficients without the Fejér summation range from –21 to 36 m (Figure 8 (a)), that is, the range of calculation errors (57 m) does not exceed 1.3% of the elevation range in the initial DEM (4568 m). Moreover, the residuals are ±1.8 m for most of the territory (Figure 8(a) and Table 1) that is less than the absolute vertical error of the SRTM DEM, 5–9 m, for this part of Africa (Farr *et al*. 2007). For the set of 7000 expansion coefficients, the residuals for the DEM reconstructed without the Fejér summation range from –11 to 15 m, that is, the range of calculation errors does not exceed 0.6% of the elevation range in the initial DEM. In this case, the residuals are ±0.8 m for most of the territory (Table 1). Thus the Fejér-free approximation can lead to much better results in terms of elevation errors compared with the approximation with the Fejér summation.

Notice that zero residuals are impossible to achieve because the polynomial series can theoretically completely converge to the original function on the Gaussian quadrature grid, which does not coincide with the DEM grid (these are errors of interpolation from the Gaussian quadrature grid to the DEM grid). Furthermore, there are unavoidable rounding errors of the computations.

On the other hand, pronounced ripple-like artifacts emerged on the maps of horizontal and vertical curvatures derived from the Fejér-free approximated DEMs (i.e., in the eastern, relatively flat part of the study area, see Figure 7(b,c)). Even for the set of 2880 expansion coefficients, one can see minor ripples in the north-eastern corner, the most flat portion of the study area (Figure 7(a)). These are oscillatory artifacts typical for approximations based on orthogonal polynomials. Classical boundary effects are also clearly visible on these maps. It is obvious that the reconstructed DEMs also include these oscillations, but they are weakly expressed and therefore cannot be seen on the elevation maps (but can be found on the residual maps, see Figure 8). Differentiation amplifies their manifestation on the curvature maps (Florinsky 2002). At the same time, these artifacts do not appear on the curvature maps if the DEM approximation included

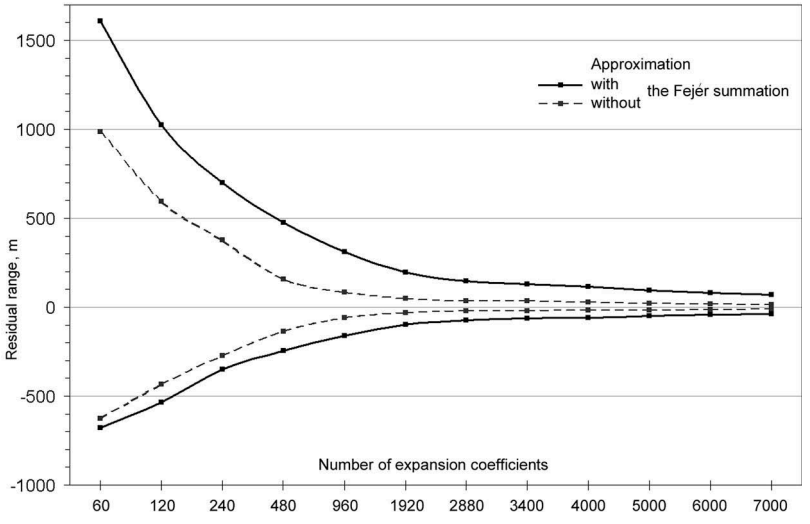

Figure 9. Convergence rate for the DEM approximation with and without the Fejér summation in terms of the residual range.

the Fejér summation (cf. Figures 3(b,d,e) and 4(b,d,e) with Figure 7). Thus the Fejér summation, suppressing this computational noise, is the absolutely necessary stage of the described method.

From the test results presented in Table 2, it is clearly seen that the time for the DEM reconstruction and calculation of a local morphometric variable depends non-linearly on the number of expansion coefficients utilized. In a small number of expansion coefficients (≤500), roughly the same time is used for both the DEM reconstruction (Equations 22–24) and the morphometric variable calculation (Equations 22, 23, 25, and 26). With increasing number of expansion coefficients (>500), the time for the morphometric calculation is sharply increased: it is about twice the time for the DEM reconstruction. It is obvious that solutions of Equations (24 and 26) require essentially different computing resources (computer memory). Indeed, processing the Kenyan DEM with the computer mentioned in Section 4, we were able to reconstruct DEMs and calculate morphometric models using up to 6500 and 4000 expansion coefficients, respectively. To work with larger sets of expansion coefficients, we used a more powerful computer.

6. Conclusions

The results demonstrated a good performance of the presented method. It can be utilized as a universal tool for analytical treatment of DEMs including DEM global approximation, denoising, generalization, as well as calculation of the partial derivatives of elevation and local morphometric variables.

At the moment, we implemented the calculation of the first, second, and third partial derivatives of elevation. This means that all presently known local morphometric variables are easily computed. Partial derivatives of higher orders are not currently used in

geomorphometry. However, if necessary, it is trivial to implement the calculation of partial derivatives of any order within the framework of the proposed method.

Notice that the method provides a natural solution for another mathematical problem of digital terrain modeling: landscape segmentation, or landform classification. This is due to the fact that common classification schemes (e.g., the Gaussian, Efremov–Krcho, and Shary classifications – Florinsky 2012, pp. 23–30) are based on signs and values of local morphometric variables (see a review – MacMillan and Shary 2009).

The developed method is universal because it combines key mathematical procedures of digital terrain modeling. The method is spectral because a set of expansion coefficients by an orthogonal basis is called 'spectrum' in functional analysis. The method is analytical because: (1) a single analytical function defines elevations within the entire study area; and (2) each calculated partial derivative of elevation is defined by a single analytical function for the entire study area. This is the fundamental difference of the presented method from the traditional techniques for DEM processing, in which one uses a DEM – a discrete function of elevation – to calculate discrete functions of the partial derivatives.

The developed method can become an effective alternative to common techniques of DTM processing. A further development of the method may include: (1) its generalization to other polynomial bases, such as the Fourier, Legendre, Bernstein, and spherical polynomials; (2) their comparative analysis in terms of efficiency and accuracy; (3) implementation of a fast recurrence algorithm (Pankratov *et al*. 2011) for calculating the expansion coefficients; (4) development of a technique to evaluate method's accuracy using metrics of numerical analysis (e.g., condition number) or statistics (e.g., root mean square error of a function of measured values); (5) comparison of the developed method with traditional techniques applied in digital terrain modeling; and (6) implementation of algorithms for solving differential equations and integral calculation, which can be used to compute nonlocal and combined morphometric variables (e.g., specific catchment area – Gallant and Hutchinson 2011).

Acknowledgement

The study was supported by RFBR grant 15-07-02484. The authors are grateful to Dr. I. Evans for the detailed review of the manuscript.

Disclosure statement

No potential conflict of interest was reported by the authors.

Funding

This work was supported by the Russian Foundation for Basic Research (RFBR) [15-07-02484].

ORCID

I. V. Florinsky http://orcid.org/0000-0003-1273-5912
A. N. Pankratov http://orcid.org/0000-0002-1503-0961

References

Arrell, K., *et al*., 2008. Spectral filtering as a method of visualising and removing striped artefacts in digital elevation data. *Earth Surface Processes and Landforms*, 33 (6), 943–961. doi:10.1002/esp.1597

Becker, J.J., *et al*., 2009. Global bathymetry and elevation data at 30 arc seconds resolution: SRTM30_PLUS. *Marine Geodesy*, 32 (4), 355–371. doi:10.1080/01490410903297766

Bergbauer, S., Mukerji, T., and Hennings, P., 2003. Improving curvature analyses of deformed horizons using scale-dependent filtering techniques. *American Association of Petroleum Geologists Bulletin*, 87 (8), 1255–1272. doi:10.1306/0319032001101

Bjørke, J.T. and Nilsen, S., 2003. Wavelets applied to simplification of digital terrain models. *International Journal of Geographical Information Science*, 17 (7), 601–621. doi:10.1080/1365881031000135500

Britenkov, A.K. and Pankratov, A.N., 2004. Stable algorithms of adaptive approximation for acoustic signals description by orthogonal polynomials. *Physics of Wave Phenomena*, 12 (3), 168–174.

Chorley, R.J. and Haggett, P., 1965. Trend-surface mapping in geographical research. *Transactions of the Institute of British Geographers*, 37, 47–67. doi:10.2307/621689

Chorowicz, J., 2005. The East African rift system. *Journal of African Earth Sciences*, 43 (1–3), 379–410. doi:10.1016/j.jafrearsci.2005.07.019

Clenshaw, C.W. and Hayes, J.G., 1965. Curve and surface fitting. *IMA Journal of Applied Mathematics*, 1 (2), 164–183. doi:10.1093/imamat/1.2.164

Courant, R. and Hilbert, D., 1989. *Methods of mathematical physics*. Vol. 1, New York, NY: Wiley.

Davis, J.C., 2002. *Statistics and data analysis in geology*. 3rd ed. New York, NY: Wiley.

Dedus, A.F., *et al*., 1995. Generalized spectral-analytic method. Part I. Theoretical foundations. *Proceedings of SPIE*, 2363, 109–112. doi:10.1117/12.199620

Dedus, F.F. *et al*., 1999. *Generalized spectral analytical method for data set processing. Problems of image analysis and pattern recognition*. Moscow: Mashinostroenie. (in Russian, with English abstract).

Dedus, F.F. *et al*., 2004. *Classical orthogonal bases in problems of analytical description and processing of information signals*. Moscow: Moscow State University Press (in Russian).

Dedus, F.F., Makhortykh, S.A., and Ustinin, M.N., 1995. Generalized spectral-analytic method. Part II. Applications. *Proceedings of SPIE*, 2363, 113–118. doi:10.1117/12.199621

Dedus, F.F., Makhortykh, S.A., and Ustinin, M.N., 2002. Application of the generalized spectral-analytic method in information problems. *Pattern Recognition and Image Analysis*, 12 (4), 429–437.

Evans, I.S., 1979. *Statistical characterization of altitude matrices by computer. An integrated system of terrain analysis and slope mapping. The final report on grant DA-ERO-591-73-G0040*. University of Durham.

Evans, I.S., 1980. An integrated system of terrain analysis and slope mapping. *Zeitschrift für Geomorphologie, Suppl*, 36, 274–295.

Evans, I.S., 2013. Land surface derivatives: History, calculation and further development. *In*: *Proceedings of Geomorphometry* 2013, 16–20 October 2013 Nanjing, paper #K-3, http://geomorphometry.org/Evans2013

Farr, T.G., *et al*., 2007. The Shuttle Radar Topography Mission. *Reviews of Geophysics*, 45 (2), RG2004. doi:10.1029/2005RG000183

Florinsky, I.V., 1998. Derivation of topographic variables from a digital elevation model given by a spheroidal trapezoidal grid. *International Journal of Geographical Information Science*, 12 (8), 829–852. doi:10.1080/136588198241527

Florinsky, I.V., 2002. Errors of signal processing in digital terrain modelling. *International Journal of Geographical Information Science*, 16 (5), 475–501. doi:10.1080/13658810210129139

Florinsky, I.V., 2009. Computation of the third-order partial derivatives from a digital elevation model. *International Journal of Geographical Information Science*, 23 (2), 213–231. doi:10.1080/13658810802527499

Florinsky, I.V., 2012. *Digital terrain analysis in soil science and geology*. Amsterdam: Academic Press.

Florinsky, I.V. and Pankratov, A.N., 2015. Digital terrain modeling with orthogonal polynomials. *Machine Learning and Data Analysis*, 1 (12), 1647–1659. doi:10.21469/22233792.1.12.01

Fox, L. and Parker, I.B., 1968. *Chebyshev polynomials in numerical analysis*. London: Oxford University Press.

Gallant, J.C. and Hutchinson, M.F., 2011. A differential equation for specific catchment area. *Water Resources Research*, 47 (5), W05535. doi:10.1029/2009WR008540

Gautschi, W., 2004. *Orthogonal polynomials: computation and approximation*. Oxford: Oxford University Press.

Golyandina, N.E., Usevich, K.D., and Florinsky, I.V., 2007. Filtering of digital terrain models by two-dimensional singular spectrum analysis. *International Journal of Ecology and Development*, 8 (F07), 81–94.

Harrison, J.M. and Lo, C.-P., 1996. PC-based two-dimensional discrete Fourier transform programs for terrain analysis. *Computers & Geosciences*, 22 (4), 419–424. doi:10.1016/0098-3004(95)00104-2

Heifetz, B.S., 1964. Approximation of the topographic surface by the Chebyshev orthogonal polynomials. *Izvestiya Vuzov, Geodesia i Aerofotosyemka*, 2, 78–86 (in Russian).

Hengl, T. and Reuter, H.I., eds., 2009. *Geomorphometry: concepts, software, applications*. Amsterdam: Elsevier.

Hutchinson, M.F., 2008. Adding the Z dimension. *In*: J.P. Wilson and A.S. Fotheringham, eds. *The handbook of geographic information science*. Oxford: Blackwell, 144–168. doi:10.1002/9780470690819.ch8

Jerri, A.J., 1998. *The Gibbs phenomenon in Fourier analysis, splines and wavelet approximations*. Boston, MA: Kluwer. doi:10.1007/978-1-4757-2847-7

Kulikova, L.I., 2007. *Spectral analytical methods for data processing and pattern recognition*. Thesis (PhD). Computing Centre, Russian Academy of Sciences (in Russian).

Li, Z., Zhu, Q., and Gold, C., 2005. *Digital terrain modeling: principles and methodology*. New York, NY: CRC Press.

MacMillan, R.A. and Shary, P.A., 2009. Landforms and landform elements in geomorphometry. *In*: T. Hengl and H.I. Reuter, eds. *Geomorphometry: concepts, software, applications*. Amsterdam: Elsevier, 227–254. doi:10.1016/S0166-2481(08)00009-3

McCullagh, M.J., 1988. Terrain and surface modelling systems: theory and practice. *The Photogrammetric Record*, 12 (72), 747–779. doi:10.1111/j.1477-9730.1988.tb00627.x

Minár, J., *et al*., 2013. Third-order geomorphometric variables (derivatives): definition, computation and utilization of changes of curvatures. *International Journal of Geographical Information Science*, 27 (7), 1381–1402. doi:10.1080/13658816.2013.792113

Mitas, L. and Mitasova, H., 1999. Spatial interpolation. *In*: P. Longley *et al*., eds. *Geographical information systems: principles, techniques, management and applications*. 2nd abr ed. Hoboken, NJ: Wiley, 481–492.

Mitášová, H. and Mitáš, L., 1993. Interpolation by regularized spline with tension: I. Theory and implementation. *Mathematical Geology*, 25 (6), 641–655. doi:10.1007/BF00893171

Pankratov, A.N., 2004a. *Algebraic operations over orthogonal series in problems of data processing*. Thesis (PhD). Institute of Mathematical Problems of Biology, Russian Academy of Sciences (in Russian).

Pankratov, A.N., 2004b. On the implementation of algebraic operations on orthogonal function series. *Computational Mathematics and Mathematical Physics*, 44 (12), 2017–2023.

Pankratov, A.N. *et al*., 2011. *Algorithms of spectral analysis using Intel IPP and MKL libraries*. Moscow: Intel – Moscow State University. (in Russian).

Pankratov, A.N. and Britenkov, A.K., 2004. Generalized spectral analytical method: problems of description of digital data by families of orthogonal polynomials. *Vestnik of the Lobachevsky Nizhni Novgorod State University, Series Radiophysics*, 1 (2), 5–14. (in Russian)

Pankratov, A.N. and Kulikova, L.I., 2006. On the derivatives calculation under uniform and mean square approximation of signals. *In*: *Computer applications in scientific researches. Proceedings of the IVTN-2006 session*. Moscow: NC Group /NVK VIST, abstract #0606, http://www.ivtn.ru/2006/physmath/enter/t_pdf/tp06_06.pdf (in Russian).

Papo, H.B. and Gelbman, E., 1984. Digital terrain models for slopes and curvatures. *Photogrammetric Engineering and Remote Sensing*, 50 (6), 695–701.

Press, W.H. *et al*., 1992. *Numerical recipes in C. The art of scientific computing*. 2nd ed. Cambridge: Cambridge University Press.

Rivlin, T.J., 1974. *The Chebyshev polynomials*. New York, NY: Wiley.

Sandwell, D.T., Smith, W.H.F., and Becker, J.J., 2008. *SRTM30_PLUS V11*. San Diego, CA: Scripps Institution of Oceanography, University of California. ftp://topex.ucsd.edu/pub/srtm30_plus/

Schut, G.H., 1976. Review of interpolation methods for digital terrain models. *Canadian Surveyor*, 30 (5), 389–412.

Segu, W.P., 1985. Terrain approximation by fixed grid polynomial. *The Photogrammetric Record*, 11 (65), 581–591. doi:10.1111/j.1477-9730.1985.tb00525.x

Shary, P.A., 1995. Land surface in gravity points classification by a complete system of curvatures. *Mathematical Geology*, 27 (3), 373–390. doi:10.1007/BF02084608

Shary, P.A., Sharaya, L.S., and Mitusov, A.V., 2002. Fundamental quantitative methods of land surface analysis. *Geoderma*, 107 (1–2), 1–32. doi:10.1016/S0016-7061(01)00136-7

Tetuev, R.K. and Dedus, F.F., 2007. *Classical orthogonal polynomials. Application to data processing problems*. Pushchino: Institute of Mathematical Problems of Biology, Russian Academy of Sciences (in Russian).

Tobler, W.R., 1969. Geographical filters and their inverses. *Geographical Analysis*, 1 (3), 234–253. doi:10.1111/j.1538-4632.1969.tb00621.x

Van Rossel, J., 1972. Digital hypsographic map compilation. *Photogrammetric Engineering*, 38 (11), 1106–1116.

Watson, D., 1992. *Contouring: a guide to the analysis and display of spatial data*. Oxford: Pergamon Press.

Wilson, J.P. and Gallant, J.C., eds., 2000. *Terrain analysis: principles and applications*. New York, NY: Wiley.

Wood, J.D., 1996. *The geomorphological characterisation of digital elevation models*. Thesis (PhD). University of Leicester.

Wu, F., 2003. Scale-dependent representations of relief based on wavelet analysis. *Geo-Spatial Information Science*, 6 (1), 66–69. doi:10.1007/BF02826705

Yagodina, L.L., 1972. Modelling of the topographic field by the Chebyshev orthogonal polynomials. *Vestnik of the Leningrad State University, Geographical Series*, 24 (4), 136–142 (in Russian, with English abstract).

Zevenbergen, L.W. and Thorne, C.R., 1987. Quantitative analysis of land surface topography. *Earth Surface Processes and Landforms*, 12 (1), 47–56. doi:10.1002/esp.3290120107